Phase II-Upgrade for ATLAS: Small-diameter Muon Drift Tubes

Daphne Blumin[1]

[1]University of Michigan Ann Arbor, MI, 48104
[2]The ATLAS group at the University of Michigan

May 2, 2021

Abstract

The upgrade of the Large Hadron Collider (LHC) to the High-Luminosity LHC (HL-LHC) will provide an unprecedented opportunity for studying electroweak symmetry breaking. One of the goals of this upgrade is to introduce new components with the aim of delivering an integrated luminosity of 300 1/fb by the end of Run 3 in 2023. Small Muon Drift Tube chambers are essential in achieving this. I will discuss in detail the Phase-II upgrade and its implications. An overview of the design and production of the new ATLAS sMDT chambers and their performance and their mechanical integration with the RPCs will be explained. Additionally, I will discuss the implications of the upgrade's ability to study Higgs-Boson coupling as well as improve our understanding beyond the standard model. sMDT, LHC, ATLAS, Muon, Higgs-Boson.

1 Introduction

The LHC recreates conditions from when the universe was a billionth of a second old which was the only time with such high naturally occurring energies. The LHC does this through proton-proton collisions which occur at a center of mass energy. When collided, the protons become a myriad of elementary particles which decay further according to each particle's lifetime. In addition, new particles are created due to the direct mass-energy relation, which allows for the massive kinetic energy to be converted to mass in the form of new particles. The lifetime of different particles is guided by the energy-time uncertainty principle given by Heisenberg:

$$\Delta E \Delta t < \hbar \tag{1}$$

The decay can, theoretically, occur in an infinite number of ways, however quantum field theory guides the probability of all possible collision results. Feynman diagrams may be used for simplicity. Muon signatures are an integral part of the

ATLAS project at the HL-LHC, which will investigate electroweak symmetry breaking through the precise measurement of the Higgs Boson couplings, which in turn requires a precise measurement of the Higgs-Boson branching ratios into different decay channels. The study of double-Higgs production and of electroweak boson scattering is essential for the characterization of the electroweak part of the Standard Model. The luminosity of the HL-LHC is expected to be an order of magnitude larger than the original LHC luminosity. Luminosity is one of the most important parameters of a particle accelerator because it is a measurement of the number of collisions that can be produced in a detector. The ATLAS Muon Spectrometer consists of three large air-core superconducting toroidal magnets, more specifically, two endcaps and one barrel. These magnets provide a field of approximately .5T. Small-diameter Muon Drift Tube detectors provide reliable muon tracking with excellent spatial resolution and high tracking efficiency independent of the track incident angle. The deflection of muon trajectories in the bending of the magnetic field ("precision coordinate") is measured via hits in 3 layers of the monitored drift tube precision chambers.

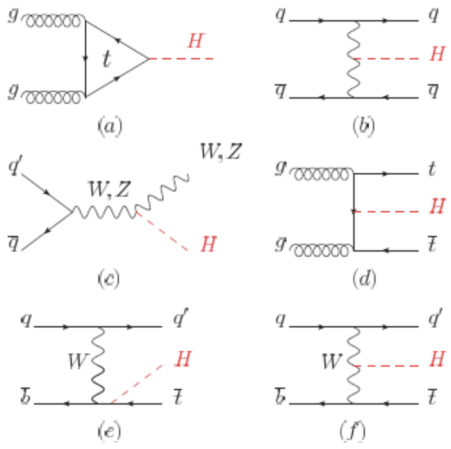

Figure 11.1: Main Leading Order Feynman diagrams contributing to the Higgs production in (a) gluon fusion, (b) Vector-boson fusion, (c) Higgs-strahlung (or associated production with a gauge boson), (d) associated production with a pair of top (or bottom) quarks, (e-f) production in association with a single top quark. with top quarks.

Figure 1: Feynman diagram for most likely Higgs-Boson decay

2 The Higgs *Field and Mechanism*

The Standard Model of particle physics is a theory that describes the known matter in terms of its elementary constituents and their interactions. It is

regarded as one of the most successful and widely proven theories in modern physics. The Standard Model (SM) of particle physics postulates the existence of a complex scalar doublet with a vacuum expectation value, which spontaneously breaks the electroweak symmetry. As a result, this scalar field gives masses to all the massive elementary particles, and gives rise to a physical scalar known as the Higgs-Boson. A key feature of the field predicted by the Standard Model is that it would take less energy for the field to have a non-zero value than a zero value, unlike all other known fields; therefore, the Higgs field has a non-zero value (or vacuum expectation) everywhere. The Higgs-Boson is the carrier particle for the Higgs field. The more a particle interacts with the Higgs field, the higher its mass. The Higgs mechanism is essential to explain the generation mechanism of the property "mass" for gauge bosons. Without the Higgs mechanism, all bosons would be considered massless, but measurements show that the W^+, W^-, and Z^0 bosons actually have relatively large masses of around 80 GeV/c^2. The Higgs field resolves this conundrum. The simplest description of the mechanism adds a quantum field (the Higgs field) that permeates all space. Below some extremely high temperature, the field causes spontaneous symmetry breaking during interactions. The breaking of symmetry triggers the Higgs mechanism, causing the bosons it interacts with to have mass. The phrase *Higgs Mechanism* refers specifically to the generation of masses for the W±, and Z weak gauge bosons through electroweak symmetry breaking. The Higgs field, through the interactions specified by its potential, induces spontaneous breaking of three out of the four generators ("directions") of the gauge group U(2). This is often written as $SU(2)_L$ X $U(1)_Y$ (which is, strictly speaking, only the same on the level of infinitesimal symmetries) because the diagonal phase factor also acts on other fields – quarks in particular. However, after symmetry breaking, these three of the four degrees of freedom in the Higgs field mix with the three W and Z bosons (W^+, W^- and Z^0), and are only observable as components of these weak bosons, which are made massive by their inclusion; the single remaining degree of freedom becomes a new scalar particle: the Higgs-Boson. There are only a few Higgs production mechanisms which lead to detectable cross sections at the LHC. Each of them makes use of the preference of the SM Higgs to couple to heavy particles: either massive vector bosons (W and Z) or massive quarks (especially t-quarks). Standard Model production of the Higgs boson at the LHC is dominated by the gluon fusion process (ggF), followed by the vector-boson fusion process (VBF). Associated production also have sizeable contributions, with a W or Z boson (VH) or a pair of top quarks (qqH). The Higgs self-interactions are defined by the Feynman rules such that the Higgs self-interaction forms can be written as:

$$g_{H^3} = 3!\lambda\nu, g_{H^4} = 4!\lambda/4 = 3M_H^2/\nu^2 \tag{2}$$

3 The Physics of The ATLAS Experiment

The ATLAS experiment relies on the beams of proton particles from the LHC colliding at the centre of the ATLAS detector. As a result of the collision, energy

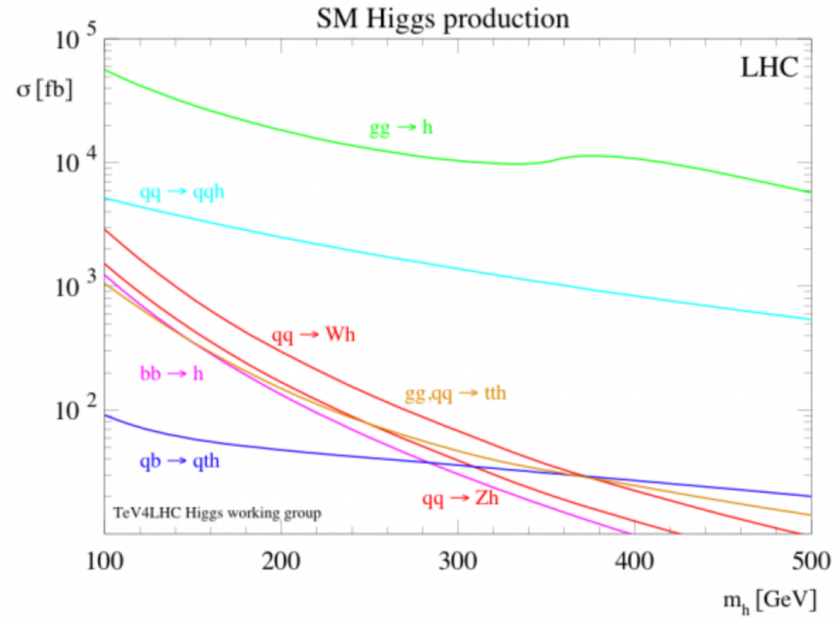

Figure 2: Illustration of the Higgs production cross-section for pp collisions

in the form of a variety of different particles (with a broad range of energies) fly out from the collision point in all directions. ATLAS has six different detecting subsystems which are arranged in layers around the collision point. In order to identify all particles produced at the interaction point, the detector is designed in layers which are made up of a variety of detectors, each of which is designed to observe specific types of particles. The different traces that particles leave in each layer of the detector allow for particle identification and accurate measurements of energy and momentum. The ATLAS detector consists of a series of ever-larger concentric cylinders which are centered around the interaction point (where the proton beams from the LHC collide). It can be divided into four major parts: the Inner Detector, the Calorimeters, the Muon Spectrometer and the Magnet systems. The detectors work together in the following way: the Inner Detector tracks particles precisely, the Calorimeters measure the energy of easily stopped particles, and the Muon system makes additional measurements of highly penetrating muons. The two magnet systems bend charged particles in the Inner Detector as well as the Muon Spectrometer, thus allowing their momenta to be measured. The only established stable particles that cannot be detected directly are neutrinos; their presence is therefore inferred by measuring a momentum imbalance among detected particles. This is only possible if the detector is "hermetic", meaning it must detect all non-neutrinos produced, with no blind spots. This paper is mainly centered on the Muon Spectrometer

system, specifically, the new sMDT chambers; however, I will briefly go through the other major components of the detector below.

3.1 Inner Detectors

The basic function of the inner detectors are to track charged particles by detecting their interaction with material at discrete points, thus revealing detailed information about the types of particles and their momentum. The magnetic field surrounding the entire inner detector causes charged particles to curve; the direction of the curve reveals a particle's charge and the degree of curvature reveals its momentum. In addition, the starting points of the "tracks" yield useful information for identifying particles; for example, if a group of tracks seem to originate from a point other than the original proton–proton collision, this may be a sign that the particles came from the decay of a hadron with a bottom quark.

3.2 Calorimeters

The calorimeters are situated outside the solenoidal magnet that surrounds the Inner Detector. Their purpose is to measure the energy from particles by absorbing it. There are two basic calorimeter systems: an inner electromagnetic calorimeter and an outer hadronic calorimeter.Both are sampling calorimeters; that is, they absorb energy in high-density metal and periodically sample the shape of the resulting particle shower, inferring the energy of the original particle from this measurement. The electromagnetic (EM) calorimeter absorbs energy from particles that interact electromagnetically, which include charged particles and photons. The hadron calorimeter absorbs energy from particles that pass through the EM calorimeter, but do interact via the strong force; these particles are primarily hadrons.

3.3 Magnet Systems

The ATLAS detector uses two large superconducting magnet systems to bend charged particles so that their momenta can be measured. This bending is due to the Lorentz force, which is proportional to velocity. Since all particles produced in the LHC's proton collisions are traveling at very close to the speed of light, the force on particles of different momenta is equal. (In the theory of relativity, momentum is not linear proportional to velocity at such speeds.) Thus high-momentum particles curve very little, while low-momentum particles curve significantly; the amount of curvature can be quantified and the particle momentum can be determined from this value. The inner solenoid produces a two tesla magnetic field surrounding the Inner Detector. This high magnetic field allows even very energetic particles to curve enough for their momentum to be determined, and its nearly uniform direction and strength allow measurements to be made very precisely. Particles with momenta below roughly 400 MeV will be curved so strongly that they will loop repeatedly in the field and

most likely not be measured; however, this energy is very small compared to the several TeV of energy released in each proton collision. The outer toroidal magnetic field is produced by eight very large air-core superconducting barrel loops and two end-caps air toroidal magnets, all situated outside the calorimeters and within the muon system.

3.4 Muon Spectrometer

The Muon Spectrometer is the largest tracking system in the ATLAS experiment. It consists of three parts: (1) a magnetic field provided by three toroidal magnets, (2) a set of 1200 chambers measuring with high spatial precision the tracks of the outgoing muons, (3) a set of triggering chambers with accurate time-resolution. The extent of this sub-detector starts at a radius of 4.25 m close to the calorimeters out to the full radius of the detector (11 m). Its tremendous size is required to accurately measure the momentum of muons, which first go through all the other elements of the detector before reaching the muon spectrometer. It was designed to measure the momentum of 100 GeV muons with 3 percent accuracy and of 1 TeV muons with 10 percent accuracy. It was vital to go to the lengths of putting together such a large piece of equipment because a number of interesting physical processes can only be observed if one or more muons are detected, and because the total energy of particles in an event could not be measured if the muons were ignored. It functions similarly to the Inner Detector, with muons curving so that their momentum can be measured, albeit with a different magnetic field configuration, lower spatial precision, and a much larger volume. It also serves the function of simply identifying muons because very few particles of other types are expected to pass through the calorimeters and subsequently leave signals in the Muon Spectrometer.

4 Muon Spectrometer Upgrade and Higgs-Boson Detection

Higgs-Boson ZZ decay:

$$H \longrightarrow ZZ^* - - > (e^+e^-e^+e^-) + (\mu^+\mu^- + \mu^+\mu^-) + (\mu^+\mu^-e^+e^-) \quad (3)$$

The Phase-II upgrade centers on the fact that as the energy of the particles produced by the accelerator increases, the detectors attached to it must grow to effectively measure and stop higher-energy particles. The ATLAS muon spectrometer consists of an efficient muon trigger system and precision muon tracking chambers providing high momentum resolution up to the TeV scale. Yet, advancements in physics are constantly providing novel ways of increasing our ability to study Higgs-Boson coupling and electro-weak boson scattering. The Higgs-Boson has an incredibly short life-time, thus we are looking for bumps in data which match the expected higgs-boson decay. Considering the mass amount of "hits" on the inner detectors, it is essential to quickly decide the

importance, or lack thereof, of the data. RPC chambers do this by measuring the muon momentum using the pattern of hit strips. The importance of precise RPC chambers inevitably increases with the luminosity, hence, more must be inserted. This can only be done if MDT chambers are replaced by using sMDT tubes as MDT tubes take up too much space. The addition of sMDT chambers will significantly reduce the accidental muon trigger rate in the transition region between the barrel and endcap. In addition, the upgraded sMDT detectors contain record sense wire positioning and have been built to cope with higher background irradiation rates at the HL-LHC as well as future upgrades of the ATLAS muon spectrometer. There are many advantages to replacing the current MDT chambers with sMDT chambers. Considering that the space charge density inside the drift tubes are proportional to the third power of the tube radius, as a result, 15 mm diameter drift tubes show a significant gain drop at 8 times higher background rates compared to 30 mm diameter drift tubes. At the same time, the deteriorating effect of space charge fluctuations on the spatial resolution is eliminated because the drift gas is approximately linear with respect to the drift radii below 7.5 mm. At the same background rate, the small-diameter drift tubes experience 8 times lower occupancy than the 30 mm diameter MDT tubes because the maximum drift time is 4 times shorter, in addition the cross section which is exposed to radiation is two times smaller than its respective counterpart (MDT). We can see the differences in drift time and drift radius between MDT and sMDT chambers in figure 2.

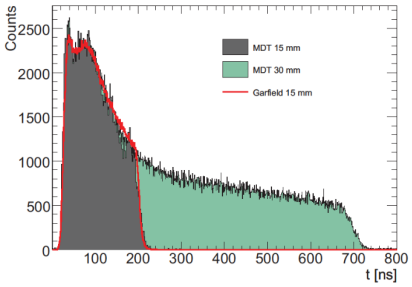

Figure 2.11: Measured drift time spectra of MDT (green) and sMDT tubes (grey), the latter compared to a GARFIELD simulation (red line) [30].

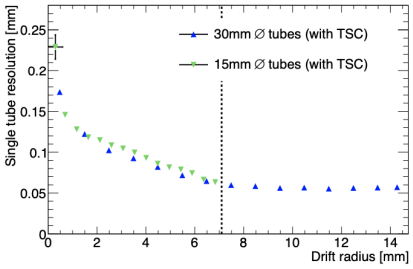

Figure 2.12: Spatial resolution after time-slewing corrections (TSC) as a function of the drift radius for MDT and sMDT drift tubes measured at the same operating conditions in the H8 muon beam at CERN without background irradiation [31–33]. As expected, the results for 15 and 30 mm diameter tubes are in good agreement for drift radii below 7.5 mm.

Figure 3: Source: ATLAS Group, CERN

A smaller cross section exposed to radiation has a much shorter drift time. This allows us to reduce the dead time to a minimum value of 220ns. In this way, the masking of muon hits by preceding background pulses is strongly reduced which increases the muon detection efficiency. This is defined as the probability to find a hit on the extrapolated muon track within 3 times the drift tube resolution. The muon spectrometer consists of several layers, all with a different purpose. The muon spectrometer consists of three large air-core superconducting toroidal magnets (two endcaps and one barrel) providing a field of approximately 0.5 T. The deflection of the muon trajectories in the bending plane of the magnetic field (the "precision coordinate") is measured via hits in three layers of monitored drift tube (MDT) precision chambers covering the region in pseudorapidity up to | η |¡ 2.7. In the innermost endcap wheels of the MS, cathode strip chambers (CSC) are used instead of MDTs in the region 2.0 ¡ | η |¡ 2.7. The muon spectrometer forms the outer part of the ATLAS detector and is designed to detect the momentum of charged particles exiting the barrel and end-cap calorimeters. This is because, unlike many particles, muons pass freely through the calorimeter. As a result, we are able to filter out much of the background particle noise and simply measure the muons, muon decay, and

elementary particles which are constantly decaying as a function of their lifetime. The precision tracking chambers in the barrel region are located between and on the eight coils of the superconducting barrel toroid magnet. In contrast, the end-cap chambers are in front as well as behind the two end-cap toroidal magnets. In the muon spectrometer, symmetry is essential; thus quality testing of every small muon drift tube is of utmost importance. The ϕ symmetry of the toroids is reflected in the symmetric structure of the muon chamber system, which consists of eight octants. Each octant is subdivided in the azimuthal direction into two sectors which have slightly different lateral extensions. One is a large sector, and the other is a small sector, leading to a region of overlap in ϕ. This overlap of the chamber boundaries minimises gaps in detector coverage and also allows for the relative alignment of adjacent sectors using tracks which are recorded by both a large and a small chamber. The chambers in the barrel are arranged in three concentric cylindrical shells around the beam axis at radii of approximately 5 m, 7.5 m, and 10 m. In the two end-cap regions, muon chambers form large wheels which are perpendicular to the z-axis. They are located at distances of $\mid z \mid \approx$ 7.4 m, 10.8 m, 14 m, and 21.5 m from the interaction point. The cross-section may be seen in figure 4.

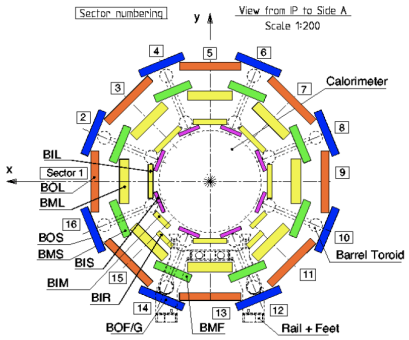

Figure 6.1: Cross-section of the barrel muon system perpendicular to the beam axis (non-bending plane), showing three concentric cylindrical layers of eight large and eight small chambers. The outer diameter is about 20 m.

Figure 4: Source: The ATLAS Group, CERN: Cross-section of barrel muon system

5 Small Muon Drift Tube: Design, Construction, Testing and Alignment

The new Small-diameter muon drift tube chambers are currently under construction at the ATLAS lab at The University of Michigan. The sMDT chambers are much less susceptible to deformation, degradation, and deterioration from space charge effects than its counterpart (MDT). In particular, at rates above 500 Hzcm^{-2}, space-charge effects deteriorate the spatial drift-tube resolution by more than 50 percent. Finally, the maximum drift time of the sMDT chambers is only 175ns as opposed to about 720 ns in the MDT chambers. Most importantly, the replacement of MDT chambers with sMDT chambers in the inner barrel (BI) allows us to add new thin-gap RPC chambers. After the phase-II upgrade, the particle fluxes will not exceed the rate capability limits of the remaining MDT chambers. In the phase-II upgrade, 16 BIS78 sMDT chambers with integrated thin-gap RPC chambers will be placed at the ends (outermost positions along the beam line, in the ATLAS-Z coordinate). This will improve the trigger efficiency and the rate capability of the chambers in the transition region between barrel and endcaps. sMDT chambers have been designed such that the construction procedures are optimized for mass production while still retaining the required accuracy. sMDT chambers are constructed using standard aluminum tubes with a diameter of 15 mm and a wall thickness of .4 mm. The ATLAS Group at The University of Michigan receives sMDT tubes which have already been assembled at Michigan State University. Prior to assembly, all of the tubes are chromatized on both the inside and outside. This ensures cleanliness as well as reliable electrical ground contact. Each drift-tube is a multi-component device that must be assembled and tested for tight quality criteria. In particular, each tube must satisfy three important requirements: correct crimping and tensioning (with tension of 350 ± 15g) of the anode wire to ensure uniformity and centrality of the wires in the aluminum tubes, low leakage current (<10 nA) to ensure noise rates below threshold, and gas pressure tightness (leak rate $< 10^{-}8$ bar L/s) to avoid changes in the drift properties of the gas.

5.1 Testing: Tube Bend

One of the most challenging aspects of constructing sMDT chambers is gravitational deformation. In order to minimize uncertainty in gravitational deformation, prior to assembly, a measurement of the raw tube bend must be taken in order to compare with MIFA measurements. According to MIFA, the industrial standards specify that the extrusion be oriented such that gravity reduces the maximum bow. Since the self bowing due to gravity of these tubes is about 1 mm, that means that the 0.5 mm specification corresponds to a bow of 1.5 mm when not influenced by gravity. A new technique has been developed to maximize precision. The setup for measuring the bending of the tube consists of a right angle aluminum bar which is inclined by an angle of 9° to prevent

the tube from rolling off. There is also a small cut-out section in the middle of the aluminum bar in order to leave only 7.5 mm of depth in the bottom part. A camera (which can magnify up to 20 times) is focused on the cut-out, such that the bottom leap of the right angle and the bottom of the tube are in direct contact. Then, by simply rotating the tube on its axis, the camera screen will eventually show a gap between the straight edge of the aluminum bar and the tube. We can then find the position of maximum bowing. Two millimeter scales are taped to the edge of the screen, which allows for one to directly read the tube bend; however, it must be noted that the zoom factor must be taken into account before recording the measured value.

We use a small digital microscope with screen and SD memory card which is pre-focused on a gap between the tube and the angle extrusion. The built in gap holder allows for easy rotation and inspection in order to measure the maximum bow. The image includes a scale for calibration which allows us to quickly judge whether the bow is .5mm or greater. Tubes which have a bow of greater than .5mm are recorded.

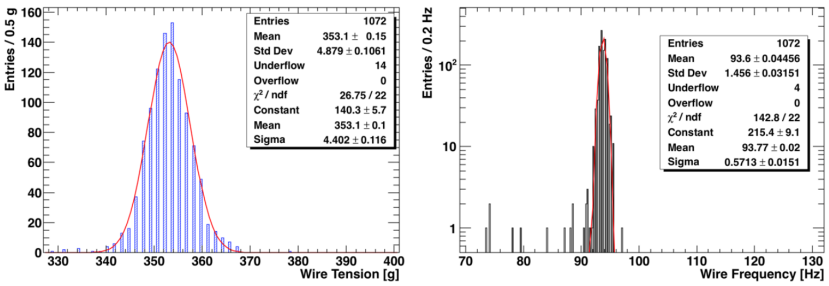

Figure 4: Tube wire tension (left) and first harmonic frequancy (right) measurements.

Figure 5: Sample tension test measurements preformed by The ATLAS Team at University of Michigan

5.2 Tension Testing

The tubes are tension tested using two 3D printed saddles, which are shaped such that one end can be pressed against a stopper. A Mitutoyo digital linear gauge (precise to ±10 micromm) is calibrated before any session of measurements with an aluminum rod whose length we know to be 1624.5 ± 0.1 mm. The tube length measurement is performed by sliding the gauge to touch the other end of the tube (endplug) and the results are shown in figure 5. The saddles are instrumented with electrical contacts, one for the outside tube aluminum cylinder to ground and another for the internal wire to have a voltage source. The mid section of the tube is immersed into a static magnetic field. Once the tube is secured and the electrical contacts on the saddles are in contact

with the wire-ends, a voltage pulse is sent through the wire, which will undergo damped transverse oscillations with frequencies given by the formula:

$$f = n/2L\sqrt{T/\rho} \rightarrow T = \pi L^2 d^2 f^2 \rho_c / g \tag{4}$$

where f is the frequency of oscillations, L and d are the wire length and diameter and ρ_c is the circular wire density, T is the tension (in grams) stretching the wire, g is the gravitational acceleration, and n is the order of the harmonic. A harmonic is any member of the harmonic series of a wave with a frequency that is a positive integer multiple of the frequency of the original wave, known as the fundamental frequency. The original wave is also called the 1st harmonic, and the following harmonics are known as higher harmonics. As all harmonics are periodic at the fundamental frequency, the sum of harmonics is also periodic at that frequency. The frequencies of these transverse oscillations are measured from the waveform of the induced Faraday current by a NI USB-6008, with an accuracy of 0.2 Hz, leading to an error on the tension of $\pm$ 0.9 g. The wire tension is required to be 350 $\pm$ 15 g. The additional sMDT tube parameters are: L = 1597 mm, d = 50 μm, $\rho_c = 19.7$ g/cm^3 and g = 9.81 m/s^2, a tension of 350 g corresponds to a (first resonant) frequency of 93.3 Hz. The tension measurement is done automatically using the LabView program, which analyzes the Fourier transform of the signal waveform. All of the measurements, each corresponding to a unique bar code, are recorded. The tubes which pass the tension test, and the tubes which fail are sorted accordingly.

5.3 High Voltage/Dark Current Testing

The dark current in this situation is the current (pedestal subtracted) measured with the tubes in the setup, caused by the current leak through the gas in the tubes, where pedestal is defined as the current measured without tubes, due to the power supply system. The setup for the dark current and high voltage tests are the same: Each tube is mounted into a test-stand and connected to a gas distribution system and the gas is then allowed to flow at a high rate (for approximately an hour) in order to flush the tubes before ramping up the HV. After the tubes are flushed they are then filled at 3 bar with the same mixture. The gas mixture used at the LHC is 93 percent Ar + 7 percent CO2; however, it is replaced with 92 percent Ar + 8 percent CO2 (still high purity) while testing individual tubes because it is much more readily available, and thus much cheaper. The tubes have already been certified at Michigan State using the proper gas and the negligible difference in performance between the two mixtures is not going to modify the results significantly. There are two separate stations used for the dark current/high voltage measurements, which in total are able to handle a total of 96 tubes. The first station is based on a commercial CAEN system which uses a SY5527 mainframe that hosts two 24 channel AG7236 HV boards, which are able to deliver up to 3.5 kV. The second testing station was made at The University of Michigan and consists of Two separate boxes which contain 8 HV boards, each of which supply 3 channels

with HV. It also measures the single tube dark current, for a total of 48 tubes. It utilizes three commercial power supplies, each able to provide up to 3kV. Both stations use a LabView based program to control the power supplies as well as to save the measurements to an external text file once every N-minutes (user chooses N). During testing, there are often a number of tubes which show dark current above the cut-off initially; however, after the first few hours with the HV turned on, often the dark current measurement comes within in an acceptable range. Sometimes the dark current increases with time, which results in a tube being marked as "bad". to a failing tube, an example of this is shown in figure 6.

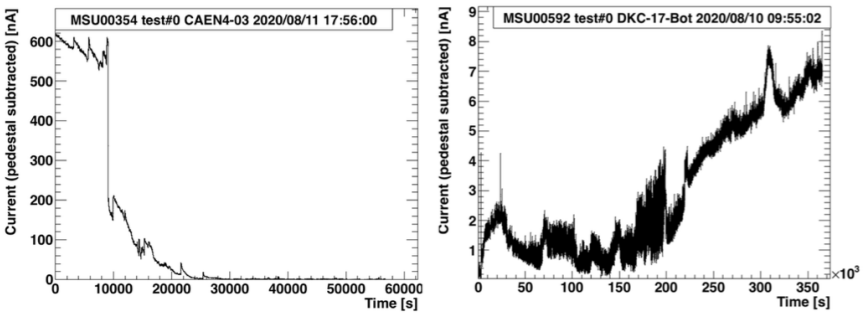

Figure 6: Example of a tube recovered from initial high dark current (left) and one that instead developed higher and higher dark current in time (right).[ATLAS Team U of M]

The procedure for the high voltage test is as follows: the high voltage is slowly raised to 2,800kV, which is above the running voltage used at the LHC (2,730 V), and the dark current is continuously measured for a few hours. A dark current value below 2 nA means the tube passed the test. If the tube measures between 2 and 5 nA, then it is left under HV to burn for a few more hours, but if the dark current does not go below the 2 nA threshold, it is rejected. Any tube whose dark current is measured to be above 5 nA is immediately rejected. The room temperature and humidity are both measured and recorded frequently because the pedestal is highly dependent on the room's humidity. Taking this into consideration, it was found that the optimal way to measure the dark current is by taking the average dark current over the last hour of testing.

6 Assembly

Once the drift tubes have passed all quality assurance tests, the chambers are assembled on a granite table in a climatized clean room. This is done by first inserting endplug reference surfaces into a grid of bores which are located in the

assembly jigs at each chamber end. The bores allow us to define the wire position of better than 5 microns. Finally, the tubes are glued to each other as well as to the spacer and support frame using an automated glue dispenser which deposits a two component epoxy glue. Constructing these chambers requires extreme precision and attention to detail. Constant attention must be paid to the spacing of the tubes and pressure used to layer them. It is important to apply pressure correctly and evenly in order to maintain symmetry and stability. After gluing each tube together, gold plated ground connection screws are inserted through holes in the jig into the triangular gaps between adjacent tube layers which are not yet filled with glue. This is done to ensure reliable electrical contact. The gaps are then filled with the glue deposited during the gluing of the next layer. Glue runs through the gaps between neighboring tubes of the next tube layer, fixing and encapsulating the ground screws. A full chamber can be completed by two researchers within approximately two days. The chambers have an in-plane alignment monitoring system which measures longitudinal sag as well as torsion between the readout and high-voltage ends of the chambers. Axial, praxial and CCC barrel alignment sensors are mounted along with the in-plane alignment system, which is on the outside of the top multilayer of all new BIS sMDT chambers in the exact same position as the present BIS MDT chambers. The BIS78 chambers also carry endcap alignment sensors on the inner multilayer in order to connect them to the NSWs. The alignment sensor platforms are mounted within 20 micron accuracy with respect to the sense wires on the outer tube layers using the precision assembly jig. It is important to measure the positions of the sense wires at both chamber ends using an automated coordinate measuring machine (CMM) with a precision of about 2 microns. An image sensor is a semiconductor device that can convert optical images into digital signals. CMOS sensors work through the photoelectric conversion function of a photoelectric device to convert the light image on the photosensitive surface into an electric signal proportional to that of the light image. This electric signal is then passed through an analog-to-digital converter which forms a digital electronic representation of the scene imaged by the sensor. The CMOS image sensor element array structure is composed of a horizontal shift register, a vertical shift register, and a CMOS image element sensitive element array. This array can then be broken down into coordinate positions, allowing for a quick and easy test for precision. Consistent measurements of alignment are preformed to ensure that symmetry and precision remain consistent despite gravitational sag or significant deformation of any kind. Overall, the optimal wire-positioning accuracy should be approximately 5 microns; however currently, on average it is about 7 microns.

7 Implications

The implications of the HL-LHC are wide ranging and exciting. The discovery of the Higgs-Boson assured physicists that the foundation upon which the standard model rests remains strong. This allows us to consider what the next

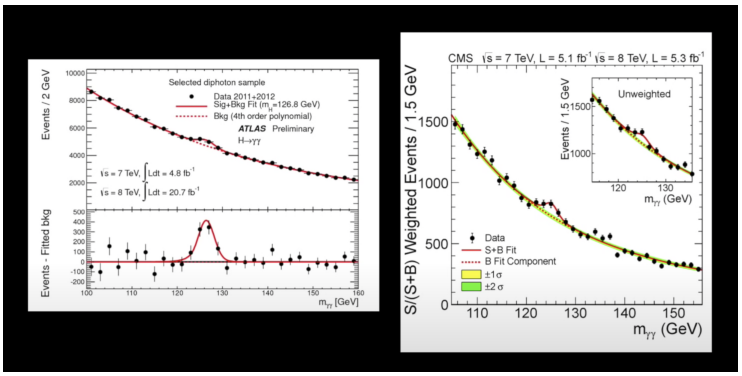

Figure 7: Higgs-Boson discovery data "bump" (ATLAS Collaberation)

discovery will be and focus our resources on studying some of the most confounding aspects of particle physics. Supersymmetry has been hailed as the most logical explanation for some of the most pressing questions in particle physics. Supersymmetry states that mass (fermions) and force (bosons) particles can not exist without each other. Supersymmetry has the potential to stabilize the gauge hierarchy, provide dark matter candidates as well as unify the electromagnetic, strong and weak forces (electroweak symmetry). The capabilities of the LHC after the phase-II upgrade may finally allow us to either confirm or deny the theory of supersymmetry. We can search for events with multijets, missing transverse momentum and 0 or 1 leptons as well as the spin correlation between top and stop quarks and electroweak gauginos.

References

[1] "sMDT Drift Tube Test Manual", The ATLAS Collaboration, University of Michigan, 2021

[2] "Higgs Production at the LHC: an Update on Cross Sections and Branching Ratios", Z. Kunszta, S. Morettib and W. J. Stirling

[3] "Higgs Production by Gluon Fusion in New Physics", Da Wei, Lin

[4] "ATLAS Muon Spectrometer Phase-II Upgrade Technical Design Report", The ATLAS Collaberation, 2017

[5] "Higgs physics: It ain't over till it is over", Sally Dawson, Christoph Englert, Tilman Plehn, 2018

[6] P.W. Higgs, Phys. Rev. Lett. 13 (1964) 508, [160(1964)].